METABONOMIC STUDY OF AMYOTROPHIC LATERAL SCLEROSIS IN SOD1G93A MOUSE MODEL

AW CHIU CHEONG
(B.Sc (Hons.), NTU)

A THESIS SUBMITTED
FOR THE DEGREE OF MASTER OF SCIENCE

DEPARTMENT OF PHARMACY

NATIONAL UNIVERSITY OF SINGAPORE

2014

DECLARATION

I hereby declare that this thesis is my original work and it has been written by me in its entirety. I have duly acknowledged all the sources of information which have been used in the thesis.

This thesis has also not been submitted for any degree in any university previously.

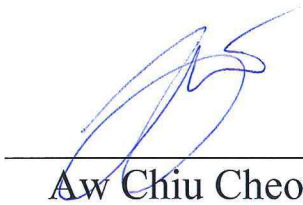

Aw Chiu Cheong
15 August 2014

Acknowledgements

I would like firstly to thank GlaxoSmithKline (GSK), Neurosciences TAU, Neural Pathways DPU (Biopolis, Singapore) for supporting this Masters Course. Without which, completing a graduate course while supporting a family with full-time employment is going to be unimaginable. Accessibility to and availability of in vivo samples, highly advanced and updated software definitely made my life easier.

I am also very grateful for having very supportive team mates in GSK DMPK whom showed understanding to me occupying freezer space, and being away at times; be it attending lectures, going for assignment discussions or running my experiments in NUS.

Taking up of a Master Course would not be possible without Dr. Eric Chan (Department of Pharmacy, NUS) if not for him taking up my candidature despite his increasing busy work schedule and rising popularity with graduate students. Sincerely appreciate his advices on experimental designs, assistance in my thesis write-up and facilitation to get administrative procedures sorted. Not forgetting the members of the Metabolic Profiling Research Group (MPRG). Especially James, Lee Cheng, Lian Yee and Yanjun (in alphabetical order), whom I would like to show my appreciation, for guiding me along in the lab, sharing protocols, looking for reagents, changing the fast-depleting nitrogen cylinder, among others.

A special shout-out to 2 GSK colleagues: May, for her assistance on getting the animal acquiring sorted patiently and of course for her delicate tissue dissection; Kishore, for being a mentor from designing of study, guidance on processing and interpretation of data, to proof-reading my thesis.

And of course Dr. Edward Browne, my manager in GSK, mustn't be missed, for I am indebted to him for his full support on my graduate study. He pushed for my sponsorship, supported my purchase of animals and consumables, approved my time-off for lessons and experiments.

Lastly, and very importantly, I am very appreciative of the support given by my loving wife. For tucking the kids into bed so that I can get some peace to work at night, for fetching the children when I need to be home late, for the tidbits so that I don't fall asleep ploughing through publications in the wee hours.

Table of Contents

Summary

Amyotrophic Lateral Sclerosis (ALS), the most common of the Motor Neuron Diseases (MND), is characterized by the progressive degeneration of the upper and lower motor neurons. Death ensues in 3-5 years from diagnosis, which consists of scoring and a physical examination to rule out other motor disorders. Riluzole is the only drug approved so far and it offers only a modest 2-3 months of extension of life with little symptomatic relief. The search for an effective therapy is a daunting uphill task with numerous agents failing in clinical trials despite showing efficacy in the preclinical disease endpoints. Using Gas Chromatography/Time-Of-Flight Mass Spectrometry (GC/TOFMS) as the analytical platform, we conducted an untargeted metabonomic profile study, to identify potential metabolites in the blood samples of SOD1G93A mouse model of ALS that can potentially serve as biomarkers to aid preclinical development of interventions. In all, 479 putative metabolite peaks were detected in the blood samples by the GC/TOFMS. After subjecting the data to PLS-DA, by applying a criterion of VIP value of more than 1.2, 95 metabolite peaks were selected as marker metabolites that separate SOD1G93A Tg mice and their matched controls. By applying further selection criteria of CV% < 30% and $p < 0.05$ using Welch's T-test, we present a panel of metabolites that cover some of the hallmark pathways of the disease, ranging from energy metabolism to mitochondria health. Sharing common pathways and specific metabolites with a clinical metabonomic study, our study offers opportunity for the development of translatable approaches to measuring drug efficacy preclinically.

List of Tables

List of Figures

1. Introduction

1.1 Amyotrophic Lateral Sclerosis

Amyotrophic Lateral Sclerosis (ALS), the most common of the Motor Neuron Diseases (MND) [1], is characterized by the progressive degeneration of the upper and lower motor neurons. Upper motor neurons include neurons that are located in the motor region of the cerebral cortex or the brain stem that carry movement information through a common pathway to the lower motor neurons in the brain stem and spinal cord that connect directly to muscles. As the disease progresses, at some point, the motor neurons can no longer send signals to the muscles leading to muscle weakening and eventual atrophy resulting in paralysis. ALS begins in the limbs, usually the arms, in about two-thirds of patients. The first symptoms are most often unilateral and focal. Early findings include foot drop, difficulty walking, and loss of hand dexterity or weakness when lifting the arms. As limb function deteriorates, patients become dependent on caregivers. Death of the patient ensues in 3-5 year after diagnosis usually due to the ultimate failure of the patient's respiratory system [2]. Incidence rates for ALS range from 1.2 - 4.0 in 100,000 person per year in Caucasians [3-6]. The incidence rates increase with age, peaking between 70 and 80 years, and are higher in men than women [7].

ALS is diagnosed based on the medical, as well as the family history of the patient, and the physical examination of the patient. It can be difficult to diagnose ALS because symptoms can vary among individuals. The disease is clinically heterogeneous even among family members harboring the same gene mutation; a single etiology can lead to numerous clinical syndromes. A combination of electromyography (EMG) and nerve conduction tests is

used for diagnosis.

ALS is classified into familial ALS (FALS) and sporadic ALS (SALS), with FALS making up approximately 10% of all ALS cases. It has been almost 150 years since Jean-Martin Charcot first described the disease in the 1860s [8]. While ALS is nearly as mysterious today as it was in the first part of the 20th century, recent breakthroughs in understanding FALS have led to new hypotheses for disease triggers and mechanisms of propagation [9, 10]. Known mutations now account for much of the rare instances of inherited ALS with mutations in the human superoxide dismutase 1 (SOD1) gene making up a large part of the FALS cases [11], other causative genes including C9ORF72 [12], *TDP43, FUS* and *OPTN,* have recently been suggested to be involved as well [9, 10]. SALS is also thought to have both genetic and environmental influences, but the principal causes await discovery [9, 10].

1.2 ALS Drug Discovery, Disease Model and Clinical Study

Riluzole was approved by the FDA in 1996 for the treatment of ALS and remains the only therapy available today. Riluzole possesses anti-glutamatergic properties that reduces excitotoxicity in ALS, providing a modest 2-3 months of life extension, however without symptomatic relief [13]. Moreover, riluzole yields side effects like diarrhea, dizziness, fatigue, nausea, and somnolence. 17 years and numerous clinical trials later, there is still no emergence of a disease-modifying treatment for ALS [14]. The lethal prognosis and the absence of effective treatments for ALS meant that all care given to patients is palliative [15].

In 1994, Gurney and colleagues created the SOD1G93A transgenic mouse line, which carries a mutant human SOD1 cDNA inserted into the mouse genome [16]. These mice carry a causative mutation (a glycine-to-alanine change at residue 93) in an array of ~25 copies of the human transgene, with the mutant human protein causing a toxic gain of function and recapitulate many features of ALS, including axonal and mitochondrial dysfunction, progressive neuromuscular dysfunction, gliosis and motor neuron loss [16, 17]. The model has an onset of paralysis at ~90 days, accompanied by degenerative changes to motor neurons that compare well with human ALS pathology [18], and death by ~135 days, depending on strain background as well as the actual mutation on the human SOD1 gene. The SOD1G93A mouse has been widely used for research ranging from basic molecular cell biology through to extensive drug trials. Only until recently, the mutant human SOD1G93A transgenic mouse model (the SOD1 mouse) had been the only available model of ALS to evaluate and progress candidate compounds into clinical trials.

The SOD1 mouse has been used extensively to study compounds or approaches with possible therapeutic value [19]. However the validity of this model has been questioned

because many compounds demonstrating efficacy in the mouse model were ineffective in human studies [20]. The fundamental differences between the genetic mouse model and the genetically and clinically heterogeneous human ALS population had been heavily debated [21]. In addition, the 'positive' results observed in the mouse model are often derived from inadequately powered studies in which administration of the compound began before disease onset. On the contrary, human clinical trials were typically performed in patients who had already passed the stage of disease onset.

Despite these differences, many studies have documented that there is a wide range of cytotoxic events common to the ALS mouse model and the human SALS patient, including evidences of excitotoxicity and oxidative injury, markers and genes reflecting programmed cell death, and neuroinflammation [22]. Recently 4 genetic biomarkers found in human bone marrow mesenchymal stem cells (hMSC) obtained from SALS patients are also found to be differentially and spatiotemporally expressed in the brain, spinal cord and muscle of the SOD1G93A mouse model [23]. The differential expressions were observed both at the pre-symptomatic and symptomatic stages of the disease. These results support the possibility of a molecular link between SALS and FALS and suggest common pathogenetic mechanisms involved in both types of ALS. As riluzole is effective in both the SOD1 mouse [24] and large populations of SALS patients, the well-established SOD1 mouse may continue to be applicable in our search for potential therapies for ALS before the industry is confident in adopting the newer ALS mouse models [25]. Importantly, the design of preclinical/clinical trials needs to be reconsidered so as to develop innovative methods in investigating ALS therapies. One example is the development of biomarkers that characterise the heterogeneity of ALS where they can be subsequently explored to improve the early diagnosis and the efficient clinical trials of ALS [19, 26].

As with many CNS disorders, ALS is likely to arise from the dynamic dysregulation of several gene and protein regulatory networks, and downstream metabolic pathways,

reflecting complex endogenous and exogenous perturbations of the systems biology. An overview of biochemical abnormalities associated with CNS disorders has been described [32], and findings are derived from studies often limited to quantifying a single, or a few metabolites. Therefore, the application of global metabonomic approaches could provide unprecedented insights into mechanistic understanding of ALS [33]. In addition, metabonomic analyses may provide opportunities to identify novel biomarkers for diagnosis or prognosis of ALS.

1.3 Metabonomics in the study of ALS

In contrast to classical biochemical approaches that often focus on a single biomarker, metabonomics, an emerging field of –omics, involves the collection of quantitative data on a broad series of metabolites in an attempt to gain an overall understanding of metabolism and/or metabolic dynamics associated with conditions of interest, including state of disease and drug exposure [27]. Metabonomics measures the dynamic multiparametric response of a living system's metabolome to genetic modifications or pathophysiological stimuli [28, 29]. Several terms have been used to describe the study of the metabolome, which include metabolomics, metabonomics, metabolic profiling, metabolic footprinting and metabolic fingerprinting. As mentioned in the previous section, metabonomics allows one to survey global changes in metabolic pathways and gain a holistic understanding of the changes in a biological system [30, 31], since fluctuations in the metabolome is a result of a complex interactions among the genome, transcriptome, proteome, and the environment [27, 30].

Using high-resolution proton-magnetic resonance spectroscopy (^{1}H-MRS) as the analytical platform, age-dependent alterations in the cerebral and spinal metabolic profiles of the SOD1G93A mouse model were determined [34]. In the spinal cord of the mouse, significantly decreased levels of N-acetyl aspartate (NAA) were already detected 60 days before the average disease onset. In addition, glutamine and c-aminobutyric acid concentration levels were significantly diminished at the pre-symptomatic stage of 75 days postpartum. These metabolic changes were further progressive in the course of the disease and started to involve the brainstem on day 75. ^{1}H-MRS studies of ALS in humans were performed several years before this mentioned study, demonstrating that either the concentration of NAA [35] or ratios NAA / creatine [36] and NAA / choline [37] are reduced in the motor cortex, that is in turn interpreted as evidence of neuronal loss due to ALS or MND. However, the claim of NAA being a potential biomarker for ALS/MND needs to be

taken with caution; NAA has also been said to be involved in Alzheimer's Disease (AD) [38], depression [39], Systemic Lupus Erythematosus (SLE) [40], Multiple Sclerosis (MS) [41] and even in head trauma [42].

Metabonomic research in ALS has largely employed Nuclear Magnetic Resonance / Magnetic Resonance Imaging / Magnetic Resonance Spectroscopy (NMR/MRI/MRS) as the analytical platform [34, 43, 44]. Being a non-invasive technique, NMR/MRI/MRS has a unique advantage considering the potential of translation of the analytical protocol to human patients. However, one limitation of magnetic resonance is its inability to detect a large number of metabolites due to its limited coverage of chemical space [45]. As such, there is an obvious need to detect a larger number of metabolites, so as to achieve a comprehensive understanding of the metabolic perturbation associated with the complex disease. Gas chromatography / time-of-flight mass spectrometry (GC/TOFMS) has been proven to be a potentially useful metabolic profiling platform based on its high sensitivity, peak resolution and reproducibility [46]. In addition, availability of an electron impact (EI) spectral library further facilitates the identification of diagnostic biomarkers and aids the subsequent mechanistic elucidation of pathological phenotypes [47]. The application of GC/TOFMS to study ALS has been investigated previously [48, 49]. In the first study, SALS patients were found to possess heterogeneous metabolite signatures in the cerebrospinal fluid (CSF), where the profiles of some patients were almost identical to controls [48]. However, the CSF metabolic profile of FALS patients without SOD1 mutation is less heterogeneous than that of the SALS patients [48]. The metabolome of the CSF of 17 FALS patients with a SOD1 gene mutation was found to form a separate homogeneous group [48]. A separate study done by this same group further showed that FALS patients carrying a mutation in SOD1 have characteristic patterns in the CSF metabolome that are statistically different from all ALS patients (both SALS and FALS) not carrying a SOD1 mutation [49]. In addition, subjects carrying the specific D90A mutation in SOD1 showed significant

differences in their CSF metabolome compared to all other subjects, including subjects carrying other mutations on their SOD1 gene [49]. These two human ALS studies provided the impetus for performing preclinical metabonomic profiling of ALS. This in turn fuels the search for biomarkers relevant to preclinical disease progression, in-line with the recommendations made by the European ALS/MND group in 2006 [50] and subsequently an update in 2009 [51].

The aim of our study is to ascertain biological pathways inflicted in this relentless neurodegenerative disease in the SOD1G93A mouse model of ALS, with the potential of identifying metabolites that can be used as biomarkers for tracking efficacy in preclinical drug discovery, and ideally translatable into the clinics for prognosis and diagnosis of ALS.

2. Materials and Methods

2.1 Animal Care

Male B6SJL-Tg(SOD1*G93A)1Gur/J (mice hemizygous for the G93A mutant form of human SOD1 gene; SOD1G93A), B6SJL-Tg(SOD1)2Gur/J (mice carrying the normal allele of the human SOD1 gene; SOD1) and Non-carrier (NCAR) mice were purchased from The Jackson Laboratories (Bar Harbor, ME, USA). The mice were housed five per cage in the laboratory and maintained on a 12 h dark/light cycle in a room with controlled temperature (20 ± 1°C) and humidity (45 ± 5%). Food and water were available to the mice ad libitum. All experiments were performed at the Biological Resource Centre (BRC) rodent facility, Biopolis, Singapore. All studies were conducted in accordance with the GSK Policy on the Care, Welfare and Treatment of Laboratory Animals and were reviewed the Institutional Animal Care and Use Committee either at GSK or by the ethical review process at the institution where the work was performed.

2.2 Biological Sampling for Metabolic Profiling

The animals were observed twice a week. Observations and animal weights were recorded for the monitoring of disease progression until they were sacrificed at 112 days post-partum. The mice were sacrificed by rapid decapitation and whole blood was collected and snap frozen immediately in dry ice. All collected blood was stored at -80°C till analysis.

2.3 Sample Derivatisation

Prior to metabolic profiling, 1 mL of monophasic extraction solvent of methanol was added to 100 µL of blood collected from each animal. The samples were vortex-mixed for 10 min, and then centrifuged at 14,000 x g for 10 min. Supernatant from each sample was transferred into a 15-mL silanised (with silanization solution I, Sigma-Aldrich) glass tube. The supernatants were concentrated to complete dryness at a temperature of 50°C for approximately 30 min using the Turbovap nitrogen evaporator (Caliper Life Science, Hopkinton, MA). Subsequently, 100 µL of anhydrous toluene (stored with sodium sulfate) was added to each of the dried extracts. Following 1 min of vortex-mixing, the samples were evaporated to dryness using the evaporator to ensure the complete elimination of any traces of water which might interfere with the subsequent sample derivatisation. The dried metabolic extract was derivatized first with 50 µL of methoxyamine (20 mg/mL) for 2 h at 60°C. Subsequently, 100 µL of N-Methyl-N-(trimethylsilyl) trifluoroacetamide (MSTFA) with 1% trimethylchlorosilane (TMCS) (Sigma-Aldrich) was added to the mixture and heated for 1 h at 60°C to form trimethylsilyl (TMS) derivatives. TMS derivatives were cooled, and 100 µL of each supernatant was transferred into GC vial and subjected to GC/TOFMS analysis, with the injection sequence being randomized. Quality Control (QC) samples were prepared by pooling 20 µL of derivative mix from 1 randomly selected sample from NCAR group and normal SOD1 group, and 2 randomly selected samples from the SOD1G93A group. QC samples were injected and analyzed at every 10 injections to monitor for GC/TOFMS analytical performance, and n-alkane standards ($C_{10\text{-}40}$, all even; Sigma-Aldrich) injected at the start and at the end of the sample analyses to determine the retention indices (RIs) of analyte peaks.

2.4 GC/TOFMS

GC/TOFMS analysis was performed using 7890A Gas Chromatography (Agilent Technologies, Santa Clara, CA) coupled to PEGASUS 4D Time-of-Flight Mass Spectrometer (LECO Corporation, St. Joseph, MI). A DB-1 GC column (Agilent Technologies) with a length of 23 m x 250 µm x 0.2 µm was used. Helium was used as the carrier gas at a flow rate of 1 mL/min. An injection volume of 1 µL was used and the injector split ratio was set to 1:2. The front inlet and ion source temperatures were maintained at 250 and 200 °C, respectively. The primary column temperature was kept at 60°C for 0.2 min, then increased by 5 °C/min to 125°C and further increased by 15 °C/min to 270°C where it was held for 7 min for analysis. The MS mass range was *m/z* 50−650 with an acquisition rate of 50 Hz. The detector voltage was set at 1650 V with electron energy of −70 eV. Solvent cutoff time was determined to be 8.3 min. Chromatogram acquisition, data preprocessing (i.e. baseline correction, noise reduction, deconvolution, peak area calculation and alignment of retention time to generate a consistent data matrix) [52], and preliminary analyte identification by the National Institute of Standards and Technology (NIST) library were performed using the LECO ChromaTOF software version 4.21 prior to conducting multivariate data analysis for all the sample groups. A calibration table was created using peaks imported from one of the QC injections [52]. Artifact, noise and reagent peaks were deleted and additional peaks of interest were registered. “Retention time (RT) deviation” was set at 2 s for peak alignment [52]. All the samples in the metabonomic experiment were selected as standards and “calculate standards” option was used to initiate peak integration. Similarity threshold was set at 60% and peaks with similarity index of more than 60% were assigned putative metabolite identities based on the NIST mass spectral library [52]. Peak area integrations were checked manually and reintegration was performed in instances of misalignment. Once the iterative verification process is optimally performed for all the peaks, the metabolite

peak area values were exported as '.csv' format for data normalization in Microsoft Office Excel using total chromatographic area normalization [53].

2.5 Multivariate Data Analysis

The resulting data was first processed by normalizing the peak area of each analyte against the total integral peak area of each sample using Microsoft Office Excel [53]. Coefficient of variance (CV%) was calculated for all putative metabolites using QC injections, and metabolites that gave CV% > 30 were discarded. All processed data were then mean-centered and unit-variance scaled before it was subjected to principal component analysis (PCA) using SIMCA-P (Umetrics, Umeå, Sweden) to identify clustering trend, as well as detect and exclude outliers that fall out of the Hostelling's Ellipse. Subsequent to the exclusion of sample outliers, the data were further subjected to partial least-squares-discriminant analysis (PLS-DA) for identification of discriminant metabolites that distinguish 2 sample classes. Two between-classes comparison experiments were performed: (1) between NCAR and SOD1 Tg and (2) between SOD1 Tg and SOD1G93A Tg. Variable importance in the projection (VIP) signifies the influence of the metabolites on the classification and its cutoff value was defined as 1.2. Welch's T-test was then used for statistical comparison of discriminant metabolite levels between two test groups. Comparisons showing p-value of less than 0.05 were considered to be statistically significantly different for the discriminant metabolites. The chemical identities of the marker metabolites were confirmed by cross-referencing with the Golm metabolite library[54] and the HMDB database [55] using the respective RIs of the marker metabolites.

2.6 Pathway Analysis

Putative identities of the shortlisted metabolites would be used as queries in a web-based software Metaboanalyst 2.0 (http://www.metaboanalyst.ca) [56]. Queries were entered as "Compound names" and "Mus musculus (mouse)" chosen as the species of relevance. For the pathway analysis algorithms, "Fisher's Exact Test" and "Relative-betweeness Centrality" chosen for "Over Representation Analysis" and "Pathway Topology Analysis" respectively. KEGG Pathway mapping (http://www.genome.jp/kegg/pathway.html) [57] was used to map the metabonomics data to the KEGG pathway maps, for biological interpretation of higher-level systemic functions.

3. Results

3.1 Animal health

Animals were initially scheduled to be euthanised and terminal samples to be collected on Day 120 postpartum, a general age that is defined as the advanced stage of disease progression for the BL6SJL strain mouse carrying the human SOD1 with the G93A mutation variant [16]. However, some of the 20 mice started showing impairment in the lower limbs when observed at Day 105. The decision was then made to collect the terminal samples earlier, and despite so, we were left with 18 mice when we harvested the samples on Day 112. As recorded in Table 1, 6 out of 18 mice demonstrated some form of motor impairment when samples were taken. The 6 mice were namely S0253, S0256, S0261, S0265, S0266 and S0267.

Table 1. Weight and observation of mice prior to sample collection. ALS-related observations include [a] both hind limbs impaired, and [b] left hind limb impaired while right hind limb paralysed. Secondary observations include [c] dried wound spots on tail, [d] penile prolapse, [e] wound on dorsal back and penile injury, and [f] dried wound on tail.

Mouse ID	Genotype	Weight (g)
W0001	Non-Carrier	30.73
W0002		29.27
W0003		25.92
W0004		29.28
W0005		32.38
W0006		34.26
W0007		34.48
W0008		31.60
W0009		31.24
W00010		31.91
W00011		28.73
W00012		29.58
T0001	SOD1	33.67
T0002		32.27
T0003		28.38
T0004		26.21
T0005		30.17
T0006		29.79
T0007 [c]		27.58
T0008		33.73
T0009		24.22
T00010		27.49
T00011 [d]		36.55
T00012		35.47
S0252	SOD1G93A	26.40
S0253 [a]		24.12
S0254		27.30
S0255		22.46
S0256 [a]		25.06
S0257		29.27
S0258		26.67
S0259		26.30
S0261 [a]		26.98
S0262 [f]		24.03
S0263		25.08
S0264		24.02
S0265 [a]		20.15
S0266 [b]		20.68
S0267 [a]		21.18
S0268		21.69
S0269		26.13
S0270		22.18

3.2 Multivariate Data Analysis

Close to 700 metabolite peaks were detected using GC/TOFMS, and after data preprocessing and calibration, the list narrowed to 479 metabolites. Peak area normalization was performed for each analyte against the total integral peak area of each sample. The final matrix table was imported into SIMCA-P v 13.0 for multivariate analysis. PCA showed that 4 samples were found outside the Hotelling's Eclipse in the scores plot and were considered outliers (Figure 1A). The remaining samples were subjected to PLS-DA. Clear clustering can be seen among each group with the 4 QC samples forming a tight cluster (Figure 1B). This reflected the low and acceptable analytical variations associated with sample preparation to data analysis and confirmed the readiness of the data for the subsequent data analysis [58].

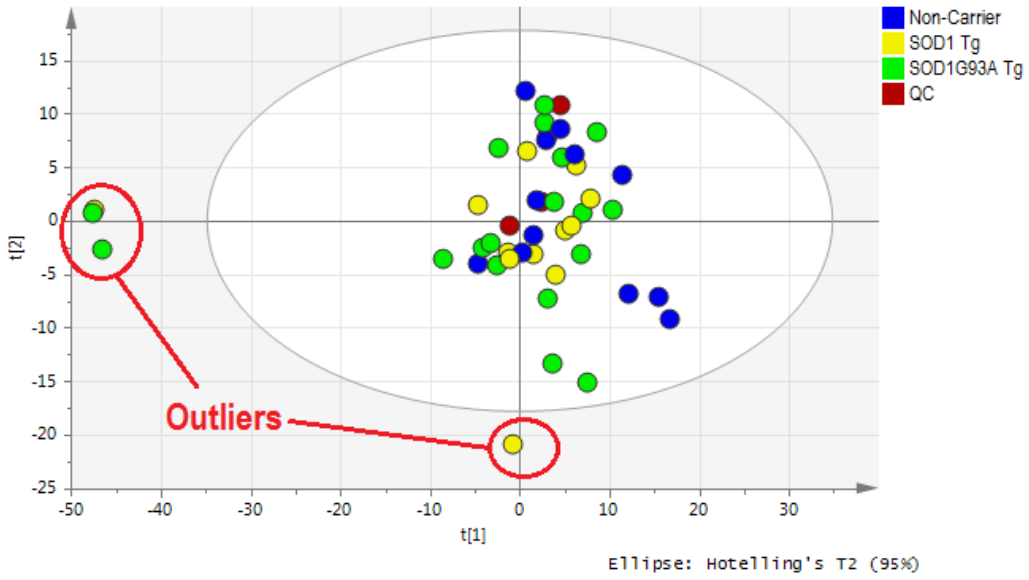

A

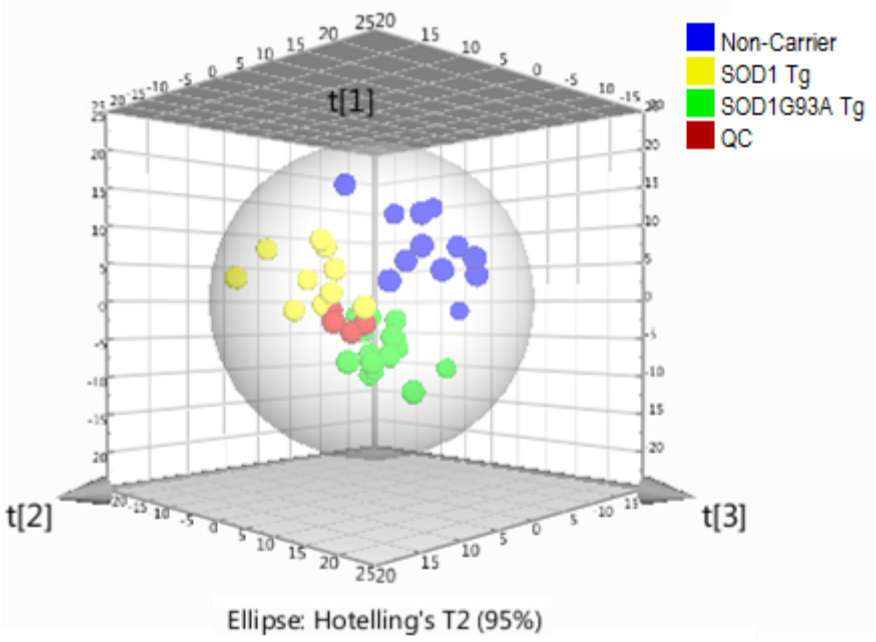

B

Figure 1. (A) PCA scores plot (R^2X=0.715, Q^2=0.48) showing 4 samples falling outside Hostelling's Ellipse. (B) PLS-DA scores plot (with the 4 outliers excluded; R^2X=0.35, R^2Y=0.513, Q^2=0.147), plotted with 3 latent variables. The QCs were tightly clustered, indicating the robustness of the sample processing and GC runs. Clear clustering of the 3 groups was observed in the PLS-DA scores plot, indicating that the metabolomes of the 3 mouse genotypes were clearly distinct.

Table 2. PLS-DA classification to investigate metabolites which define the separation between the classes in the 2 comparison sets namely (1) NCAR vs SOD1 Tg, and (2) SOD1 vs SOD1G93A Tg.

Comparison	Class 1	Class 2
1	NCAR	SOD1 Tg
2	SOD1 Tg	SOD1G93A Tg

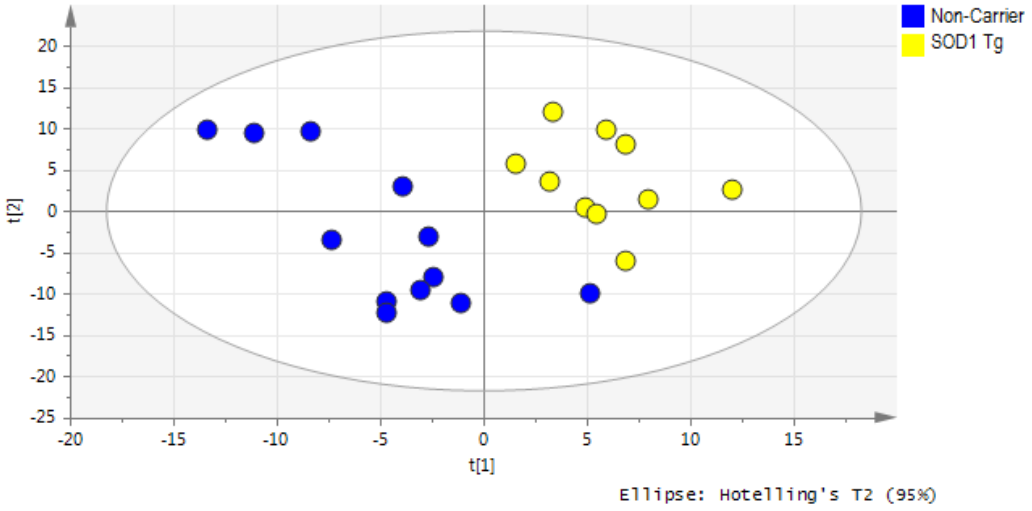

A

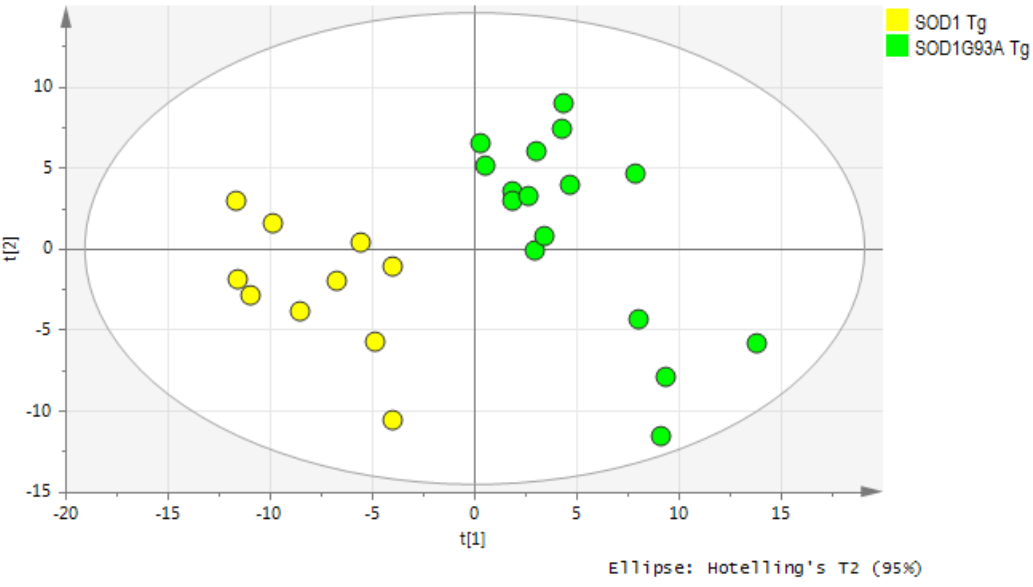

B

Figure 2. PLS-DA were performed with the classifications specified in Table 2. Clear distinctions were shown between the 2 classes in each of the 2 comparisons; (A) between Non-Carrier and SOD1 Tg mice (R^2X=0.377, R^2Y=0.957, Q^2=0.334), (B) Between SOD1 Tg and SOD1G93A Tg mice (R^2X=0.222, R^2Y=0.886, Q^2=0.504).

Samples from SOD1 Tg group and SOD1G93A Tg group were classified as class 1 and 2 respectively with all other samples excluded in Comparison 2 (Table 2) and subjected to PLS-DA. Using the criteria set as mentioned in Materials and Methods, briefly: VIP > 1.2, $p < 0.05$ and CV% in QC injections < 30%, 70 metabolites were identified to be contributing significantly to the separation between SOD1 Tg mice and SOD1G93A Tg mice in the PLS-DA. 11 of which were later excluded as they too were found to be significantly different ($p<0.05$) in Comparison 1 (between wildtype Non-Carrier and healthy SOD1 Tg mice). These 11 metabolites were differentially expressed in the 2 healthy genotypes, therefore including them into our subsequent analysis for differences in the metabolome between SOD1 Tg mice and SOD1G93A Tg mice could confound the analysis. 2 more metabolites were removed as the matched identities indicated that these 2 peaks were artifacts derived from the derivatizing agents. This resulted in 57 metabolites that contributed significantly to the difference in metabolomes of the 2 genotypes due to the mutation of the human SOD1 gene (Table 3).

Table 3. List of blood marker metabolites identified from PLS-DA of SOD1 Tg and SOD1G93A Tg mice.

Met_ID	Putative Identity (as provided in the respective source libraries)	VIP	Fold change w.r.t. Healthy control (SOD1 Tg)	Increase / Decrease	CV% in QC injections	Source of ID matches
Met_402	MyoInositol-2-phosphate **	>2.0	1.833	↑	9.13	GMD
Met_386	3-phosphoglycerate **		1.703	↓	6.06	NIST
Met_438	Isomaltose ***		1.508	↓	4.32	GMD
Met_415	Glyceric acid-1,3-diphosphate ***		2.637	↑	6.64	GMD
Met_312	9-Tetradecenoic acid ***		2.385	↓	4.67	NIST
Met_352	11-Eicosenoic acid ***		1.374	↓	4.23	NIST
Met_236	Homovanillic acid ***		1.412	↑	7.92	GMD
Met_194	5-(aminomethyl)-isoxazol-3-ol	1.5 – 2.0	1.647	↓	4.89	NIST
Met_408	Inosine		1.417	↓	3.19	NIST
Met_406	4-Ketoglucose		1.419	↓	2.61	GMD
Met_216	3-oxalo-Malic acid		1.624	↓	2.21	GMD
Met_221	Lyxonic acid-1,4-lactone		1.442	↓	9.39	GMD
Met_188	5-Methyl-acetophenone		1.110	↑	0.91	NIST
Met_403	Phthalic acid, cyclohexyl 2-pentyl ester		1.228	↑	5.61	NIST
Met_317	Hexadecanoic acid **		1.295	↓	7.15	GMD
Met_152	Methanesulfinic acid, trimethylsilyl ester **		2.885	↑	11.17	NIST
Met_171	D-mannopentadecane-1,2,3,4,5-pentaol **		1.802	↓	16.49	NIST
Met_233	4-[Acetyloxy-(2-pyridyl)methyl]-1,2-dihydro-2-oxoquinoline		1.125	↑	1.40	NIST
Met_436	Uridine 5'-monophosphate *		1.507	↑	5.83	GMD
Met_465	Cholesterol-epoxide **		1.788	↑	11.98	GMD
Met_458	4-(2,2-dimethyl-6-methylene-cyclohexyl)-butan-1-ol **		1.846	↑	2.80	NIST
Met_385	Glyceric acid-2,3-diphosphate		1.372	↓	4.33	NIST
Met_242	Oxytetradecanoic acid		3.729	↑	11.54	NIST
Met_039	9,12-Octadecadienoic acid (Z,Z)-, 2-(acetyloxy)-1-[(acetyloxy)methyl]ethyl ester		1.114	↑	3.94	NIST
Met_015	Oxalic acid **		1.651	↑	14.78	GMD
Met_135	5-Amino-2-isopropyl-1-phenyl-2,3(1H)-dihydro-pyrrole-3,3,4-tricarbonitrile		1.101	↑	1.55	NIST
Met_019	3-hydroxy-Butanoic acid		1.419	↓	4.34	GMD
Met_212	2-Hexenal, 5-(1-ethoxyethoxy)-, [R*,S*-(E)]-(.+-.)- **		1.139	↑	2.84	NIST
Met_180	1H-Indole-2,3-dione		1.526	↑	9.10	NIST
Met_225	Glycerol-2-phosphate **		1.192	↓	3.03	GMD
Met_223	Orotic acid		1.593	↑	23.71	GMD
Met_112	1,6-dimethoxy-2,4-Hexadiene		1.639	↑	9.65	NIST
Met_446	3,7-dimethyl-3-Octanol		1.110	↑	6.84	NIST
Met_290	5-Amino-3-(1-methyl-1H-pyrrol-2-yl)-1-phenyl-3-trifluoromethyl-2,3-dihydro-1H-pyrazole-4-carbonitrile		1.113	↑	3.13	NIST
Met_277	Thiocyanic acid, 2,4,6-trinitrophenyl ester		1.407	↑	2.96	NIST
Met_191	a-methyl-3-phenoxy-Benzeneacetic acid		1.708	↓	6.91	NIST
Met_252	Unknown		1.119	↑	1.32	-
Met_016	Unknown		1.425	↑	6.52	-
Met_024	Unknown **		1.462	↑	2.36	-
Met_200	Methanesulfinic acid		1.120	↑	3.46	NIST
Met_251	2-amino-3-methoxy-Benzoic acid		1.117	↑	0.83	GMD
Met_078	Glycerol	1.2 – 1.5	1.338	↓	2.92	GMD
Met_372	Xylitol		1.246	↓	5.87	NIST
Met_432	2-methoxy-2-methyl-Propane		1.138	↑	3.24	NIST
Met_267	Glucopyranose		1.583	↑	20.88	GMD
Met_389	Acetic acid		1.494	↑	3.94	NIST
Met_407	Docosahexaenoic acid, 4,7,10,13,16,19-(Z,Z,Z,Z,Z,Z)		1.186	↓	17.75	GMD

Met_332	Tetradecanoic acid	1.2 – 1.5	1.267	↓	13.92	NIST
Met_395	Uridine		1.464	↓	10.83	GMD
Met_453	Cholest-5-ene		1.243	↑	3.72	GMD/NIST
Met_199	Quinoxaline-6-carboxamide		1.752	↓	4.00	NIST
Met_268	2-ethylcyclohexanol		1.583	↑	22.88	NIST
Met_342	8,8-dimethyl-4H,8H-Benzo[e][1,2,4]-triazolo[3,4-c][1,2,4]-triazin-6(7H)-one,		1.865	↑	9.15	NIST
Met_098	Homoserine		1.465	↓	7.16	GMD
Met_464	Prost-13-en-1-oic scid		1.771	↑	4.83	NIST
Met_421	Methylmalonate		1.248	↑	14.09	NIST
Met_255	Ribonic acid		1.219	↑	3.21	NIST

All listed metabolites are identified with VIP>1.2 and found to be statistically significant with p-value of less than 0.05, calculated with Welch's T-test. The CV% of these metabolites in the pooled QC samples are less than 30%. **p<0.01, ***p<0.001.

3.3 Pathway Analysis

Among the 57 marker metabolites, 54 metabolites with putative identities were further subjected to web-based pathway analysis (Metaboanalyst) [56]. Before we could perform any functional pathway analysis, a match between the compound names provided by the library sources (NIST and GMD) and the ones in MetaboAnalyst's knowledgebase had to be established (Table 4). In some cases, there might be redundancies and conflicts due to different naming schema. The compounds with name conflicts were highlighted for subsequent manual inspection. Based on the 54 compounds names presented to the software, 40 matches were established (Table 4).

Table 4. List of metabolites input into MetaboAnalyst for pathway analysis and their corresponding matches based on MetaboAnalyst's knowledgebase.

Query	Match
MyoInositol-2-phosphate	Myo-inositol 1-phosphate
3-phosphoglycerate	3-Phosphoglyceric acid
Isomaltose	Isomaltose
Glyceric acid-1,3-diphosphate	Glyceric acid 1,3-biphosphate
9-Tetradecenoic acid	Myristoleic acid
11-Eicosenoic acid	11-Eicosenoic acid
Homovanillic acid	Homovanillic acid
5-(aminomethyl)isoxazol-3-ol	-
Inosine	Inosine
4-Ketoglucose	D-Arabino-hexos-2-ulose
3-oxalo-Malic acid	3-Oxalomalate
Lyxonic acid-1,4-lactone	Threonolactone
5-Methyl-acetophenone	2-Methylacetophenone
Phthalic acid, cyclohexyl 2-pentyl ester	-
Hexadecanoic acid	Palmitic acid
Methanesulfinic acid	-
D-mannopentadecane-1,2,3,4,5-pentaol	-
4-[Acetyloxy-(2-pyridyl)methyl]-1,2-dihydro-2-oxoquinoline	-
Uridine 5'-monophosphate	Uridine 5'-monophosphate
Cholesterol-5alpha,6beta-epoxide	-
4-(2,2-dimethyl-6-methylene-cyclohexyl)-butan-1-ol	gamma-Ionone
Glyceric acid-2,3-diphosphate	Glyceric acid 1,3-biphosphate
oxytetradecanoic acid	2-Hydroxymyristic acid
9,12-Octadecadienoic acid (Z,Z)-, 2-(acetyloxy)-1-[(acetyloxy)methyl]ethyl ester	Methyl linoleate
Oxalic acid	Oxalic acid
5-Amino-2-isopropyl-1-phenyl-2,3(1H)-dihydro-pyrrole-3,3,4-tricarbonitrile	-
3-hydroxy-Butanoic acid	3-Hydroxybutyric acid
2-Hexenal, 5-(1-ethoxyethoxy)-, [R*,S*-(E)]-(.+-.)	-
1H-Indole-2,3-dione	Indole-5,6-quinone
Glycerol-2-phosphate	Beta-Glycerophosphoric acid
Orotic acid	Orotic acid
1,6-dimethoxy-2,4-Hexadiene	-
3,7-dimethyl-3-Octanol	3,7-Dimethyl-3-octanol
5-Amino-3-(1-methyl-1H-pyrrol-2-yl)-1-phenyl-3-trifluoromethyl-2,3-dihydro-1H-pyrazole-4-carbonitrile	-
Thiocyanic acid, 2,4,6-trinitrophenyl ester	-
a-methyl-3-phenoxy Benzeneacetic acid	-
Methanesulfinic acid	S-Methyl methanesulfinothioate
2-amino-3-methoxy-Benzoic acid	-
Glycerol	Glycerol
Xylitol	D-Xylitol
2-methoxy-2-methyl-Propane	2,2-Dimethyloxirane
Glucopyranose	D-Glucose
Acetic acid	Acetic acid
Docosahexaenoic acid, 4,7,10,13,16,19-(Z,Z,Z,Z,Z,Z)	(4Z,7Z,10Z,13Z,16Z,19Z)-Docosahexaenoic acid
Tetradecanoic acid	Myristic acid
Uridine	Uridine
Cholest-5-ene	Cholest-5-ene
Quinoxaline-6-carboxamide	-
2-Ethylcyclohexanol	(+/-)-Carvomenthol
8,8-dimethyl-4H,8H-Benzo[e][1,2,4]-triazolo[3,4-c][1,2,4]-triazin-6(7H)-one	2-(4-Hydroxyphenyl)-3,6-dimethoxy-8,8-dimethyl-4H,8H-benzo[1,2-b:3,4-b']dipyran-4-one
Homoserine	L-Homoserine
Prost-13-en-1-oic scid	Prostaglandin E1
Methylmalonate	Methylmalonic acid
Ribonic acid	Ribonic acid

Identified pathways using Metaboanalyst are presented in Table 5. They included glycolysis, pentose and sucrose metabolism, fatty acids elongation and biosynthesis, among others. Kyoto Encyclopedia of Genes and Genomes, KEGG[57], is a database resource for understanding high-level functions and utilities of the biological system, such as the cell, the organism and the ecosystem, from molecular-level information, especially large-scale molecular datasets generated by genome sequencing and other high-throughput experimental technologies. KEGG PATHWAY mapping is the process to map molecular datasets, especially large-scale datasets in genomics, transcriptomics, proteomics, and metabolomics, to the KEGG pathway maps for biological interpretaion of higher-level systemic functions. Based on KEGG analysis, the pathways were further classified into 4 major functions namely, carbohydrate metabolism, lipid metabolism, nucleotide metabolism and amino acid metabolism (Table 5).

Table 5. Biological pathways and systemic functions implicated in SOD1 mutation as uncovered by global blood metabonomic profiling.

Biological Pathway	Metabolite IDs	Systemic Function
Glycolysis or Gluconeogenesis	D-glucose, Glyceric acid 1,3-biphosphate, Acetic acid, 3-phosphoglycerate	Carbohydrate Metabolism
Pentose phosphate pathway	D-glucose	
Pentose and glucuronate interconversions	D-xylitol	
Galactose metabolism	Glycerol	
Starch and sucrose metabolism	Isomaltose	
Pyruvate metabolism	Acetic acid	
Butanoate metabolism	3-Hydroxybutyric acid	
Inositol phosphate metabolism	Myo-inositol 1-phosphate	
Fatty acid metabolism	Palmitic acid	Lipid Metabolism
Fatty acid biosynthesis	Myristic acis, Palmitic acid	
Fatty acid elongation in mitochondria	Palmitic acid	
Synthesis and degradation of ketone bodies	3-Hydroxybutyric acid	
Biosynthesis of unsaturated fatty acids	Palmitic acid, Docosahexaenoic acid	
Glycerolipid metabolism	Glycerol	
Purine metabolism	Inosine	Nucleotide Metabolism
Pyrimidine metabolism	Uridine 5'-monophosphate, Orotic acid, Uridine	
Valine, leucine and isoleucine metabolism	Methylmalonic acid	Amino acid metabolism
Tyrosine metabolism	Homovanillic acid, Indole-5,6-quinone	

4. Discussion

4.1 Changes in carbohydrate metabolism

Abnormalities in carbohydrate metabolism in ALS patients have long been suggested. As early as in the 70's, ALS patients had been found to have a high incidence of diabetes, with a large proportion having abnormal glucose tolerance [59]. The latter has been recently verified to be the case even in non-diabetic ALS patients and suspected to be in association with increased levels of free fatty acids [60]. In the same year when the discovery of the G93A mutant of the human SOD1 gene in association to the disease had been published [11], investigation showed enhanced metabolism of glucose to fructose in muscle isolated from ALS patients [61]. There were also evidence that showed increased ketohexokinase activities and aldolase, which suggested that further metabolism of fructose may occur via a fructolytic pathway. In our work, high blood glucose has also been measured. Glycolysis intermediate 1,3-biphosphate glycerate has been detected at a higher level compared to the healthy SOD1 Tg control mouse, with a decrease in 3-phosphoglycerate (Table 3). These point to a reduction in ATP synthesis via the glycolytic process. Acetic acid, involved in the initiation of the Tricarboxylic Acid (TCA) cycle after its activation, has also been found to be in excess in the diseased animal (Table 3). The degeneration of motor units, composed of different kinds of motor neurons and muscles fibers, represents the first detectable event in ALS [62, 63]. Fast fatigable motor units are composed of large alpha-motor neurons and glycolytic muscle fibers that preferentially burn glucose to exert heavy force for a short period. Conversely, slow motor units correspond to small alpha-motor neurons and oxidative muscle fibers, which store and use fatty acids preferentially to produce less intense but constant strength. Large alpha-motor neurons are the first to degenerate in ALS models

[63, 64], and glycolytic motor units are preferentially affected in both ALS patients and mouse models [65-67]. The selective vulnerability of large alpha-motor neurons is potentially due to their higher energetic needs that could either be not fulfilled or a source of oxidative stress. The animals were in the advanced stage of the disease and hind limb impairment had set in (Table 1); in some there were almost complete lower limb paralysis. It is therefore likely that the glycolytic muscles in these animals had been so affected that the reduction in the glycolytic process is evident in the systemic blood circulation of the animals. In fact, even in the early stages of disease progression, the glycolytic muscles of SOD1G93A Tg mice switched toward an oxidative phenotype, presumably due to the loss of their connection to large alpha-motor neurons and subsequent reinnervation by “slow” motor neurons [68].

4.2 Hypermetabolism

Hypermetabolism has been consistently reported in ALS patients [69-72]. Patients lose some weight due to the inevitable reduction in skeletal muscle mass resulting from denervation and decreased physical activity. In most cases weight loss also has a nutritional component attributable to malnutrition, the principal cause of which is decreased dietary intake. Swallowing disorders and dysphagia affect most ALS patients. Anorexia, digestive disorders and upper extremity motor difficulties also contribute to low dietary intake. Another cause of malnutrition is an increase in energy requirements sufficient to exceed dietary intake. Reports that resting energy expenditure (REE) may be increased in this context [71, 73, 74] appear paradoxical because free fat mass (FFM), the main determinant of REE, decreases in ALS due to reasons discussed above. Kasarskis et al. [74] suggested that hypermetabolism in ALS probably reflected added energy demand due to increased respiratory work. They found that REE increased as death approached whereas forced vital capacity (FVC) declined, as did BMI and FFM. However, REE was not studied in relation to FFM, and the evolution of REE and FVC was evaluated by looking at variations between patients at different stages of disease rather than by following individual patients as they progressed. Energetic alterations are similarly found in the SOD1 transgenic mouse model of ALS. Apart from producing less ATP due to the switching off of the glycolytic process (glycolysis itself produces 2 ATP in each glucose molecule), the dysfunctional electron transport chain have also resulted in ATP synthesis taking place inefficiently [75]. These mice are leaner than controls, hypermetabolic, hypolipidemic and present increased fatty acid uptake in muscles [76, 77]. In case of higher energy needs, neurons can use ketone bodies as an energetic substrate when glycolysis can no longer sustain the ATP demand of the system [78]. In this situation, astrocytes will use lipid to provide ketone bodies to neurons, and

potentially motor neurons in ALS [79]. The blood concentration of 3-hydroxybutyric acid, the major of the 3 ketone bodies (with acetoacetate and acetone), was found to be lower in the mutant SOD1 model than that of matched controls in our current study (Table 3). At the same time, medium length fatty acids like myristic acid, palmitic acid and docosahexaenoic acid (DHA) were also found to be at lower abundance when compared against their levels in matched controls (Table 3). Therefore a similar shift from utilising glucose to using ketone bodies and fatty acids to fuel the TCA cycle was observed in the SOD1G93A mice. Encouragingly, our preclinical observations of perturbed carbohydrate and lipid metabolism corroborated with the findings of a recent clinical study that profiled blood markers associated with ALS patients when compared to disease mimic patients and healthy participants [80].

4.3 Nucleoside / Nucleotide Metabolism

Uridine is a pyrimidine nucleoside that is required for phospholipid, glycogen, and RNA synthesis [81]. The increase of orotic acid and uridine 5'-monophosphate with the decrease in level of uridine may indicate the fall in de novo synthesis of uridine (Figure 3). The fact that uridine is a key metabolite is illustrated by the rare, inherited form of the disease orotic aciduria in humans due to deficiencies of the enzyme uridine monophosphate synthetase (UMPS). This deficiency leads to mental retardation and the failure to thrive. Inherited orotic aciduria in humans is treated by uridine supplement thus bypasses the metabolic block due to UMPS dysfunction. Much of the cytidine 5'-triphosphate (CTP) utilized in the Kennedy cycle for synaptogenesis in the human brain is derived from uridine [82, 83]. The CNS uptake of uridine, the principle circulating pyrimidine, occurs from the circulation through the blood- brain barrier primarily by the sodium-dependent CNT2 nucleoside transporter [84] and enters into cells via an ATP driven uridine-UTP cycle [85] where interconversion to largely non-circulating essential compounds occurs. In the SOD1G93A mouse, uridine administration increased survival by 17.4%, ameliorated body weight loss, enhanced motor performance, reduced gross lumbar and ventral horn atrophy, attenuated lumbar ventral horn neuronal cell death, and decreased reactive astrogliosis [86]. Uridine synthesis is located on the inner mitochodrial membrane and coupled functionally with ubiquinone. The formation of uridine requires functioning mitochondria, and uridine is necessary to support the growth of cells that lack mitochondria [87].

Purines and pyrimidines are potent signaling molecules which target a broad range of tissues and cell types [88]. The extracellular release of nucleosides and nucleoside tri-phosphates (NTPs), especially adenosine and ATP respectively, is a common feature of various cells under different conditions, such as muscle, lymphocytes, neurons and glial cells

which have prominent roles in ALS [89]. Considering that extracellular purines and pyrimidines are crucial neuron-to-microglia alarm signals in the CNS, and that ALS is the result of a multipart anomalous cellular interplay, it seems highly possible that purinergic dynamics might indeed also have a certain role in the onset and progression of ALS. Target receptors include 7 ionotropic P2X channels (P2X1–7) [90], 8 G-protein-coupled P2Y receptors (P2Y1, 2, 4, 6, 11–14) [91], 4 G-protein-coupled P1 receptors (A1, A2A, A2B, A3) [92]. A2A receptor antagonists such as preladenant, are in trial for the treatment of early Parkinson's disease (www.clinicaltrial.gov), and istradefylline (KW-6002) for Parkinson's disease symptoms and dyskinesia that develops after a long-term treatment with levodopa [93]. The P2X7 receptor has been targeted by antagonists: Pfizer's CE-224535, AstraZeneca's AZD-9056 and Evotec's EVT-401, to reduce inflammation in peripheral pathologies [94], and the potential of CNS indications is in discussion. The decrease in systemic inosine (Table 3), possibly adenosine and ATP as well, could result in a downregulation in inflammatory responses. Whether or not it is an innate defense mechanism awaits investigation. More likely, the low inosine level is a consequence of a lower ATP production (Figure 4) due to the shut down of glycolysis in the cytosol on top of the inefficient oxidative phosphorylation taking place across the mitochondrial inner membrane, along defective electron transport chain [75].

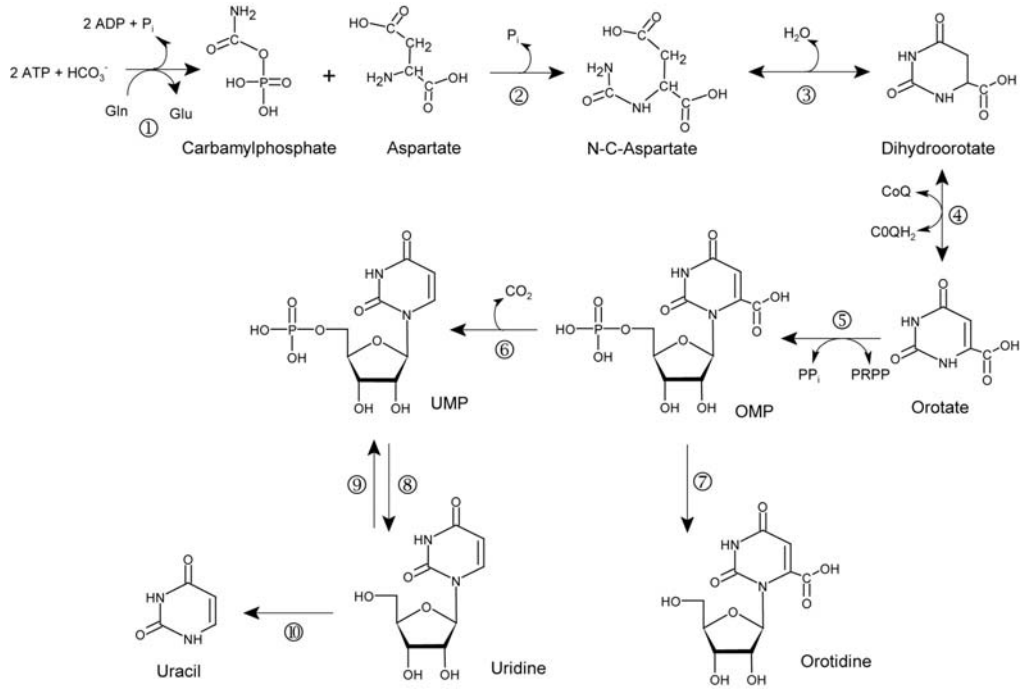

Figure 3. Pyrimidine de novo synthesis pathway [95]. 1, carbamylphosphate synthetase; 2, aspartate transcarbamylase; 3, dihydroorotase; 4, dihydroorotate dehydrogenase; 5, orotate phosphoribosyltransferase; 6, orotidine 5'-monophosphate decarboxylase; 5 + 6, UMP synthase; 7, orotidine 5'-monophosphate phosphohydrolase; 8, pyrimidine 5'-nucleotidase; 9, uridine kinase; Graphic, uridine phosphorylase.

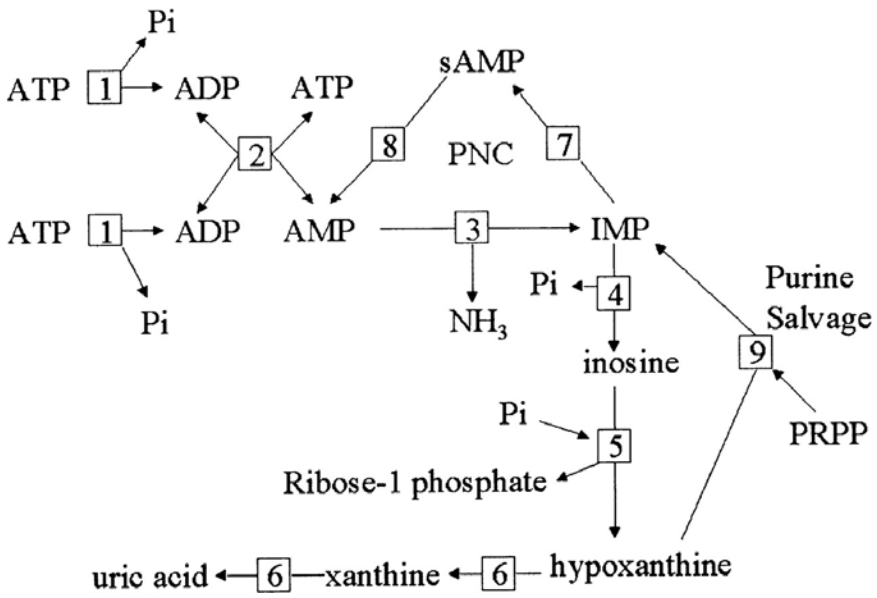

Figure 4. Biochemical pathways involved in skeletal muscle inosine monophosphate (IMP) metabolism [96]. 1, ATPase; 2, adenylate kinase; 3, AMP deaminase; 4, cytoplasmic 5'-nucleotidase; 5, purine nucleoside phosphorylase; 6, xanthine oxidase; 7, adenylosuccinate synthetase; 8, adenylosuccinate lyase; 9, hypoxanthine/guanine 5-phosphoribosyl 1-pyrophosphate (PRPP) transferase. sAMP, succinyl AMP; PNC, purine nucleotide cycle.

4.4 Dopaminergic Systems

It has been suggested that there is impairment of the central dopaminergic systems in ALS patients, thus suggesting that there is degeneration of neuroanatomical structures other than motor neurons [97]. Indeed the depletions of dopamine and homovanillic acid (HVA) were significantly greater in the striatal tissues of SODG93A Tg mice compared to their littermate control mice [98]. HVA, a breakdown product of dopamine as well as noradrenaline, has been found to be elevated in plasma under metabolic stress [99, 100]. Plasma HVA, although largely derived from the periphery, is thought to reflect, at least partly, the central dopamine response to stress [100, 101]. Indeed in our metabolic profile, HVA was significantly elevated in the blood of mice carrying the mutant human SOD1 (Table 3), indicative of dopaminergic breakdown. There were only a couple of studies published in the 1990s that investigated the association between HVA and ALS [97, 102], and after that more often than not, HVA changes have been associated with Parkinson Disease only. The involvement of the central dopaminergic system in ALS is an area that has been relatively unexplored.

5. Conclusion

The pathophysiological mechanisms underlying ALS are multifactorial, with a complex interaction between genetic factors and molecular pathways that remain to be better understood. Proposed mechanisms that are involved in the pathology of ALS include glutamate excitotoxicity, protein misfolding, oxidative stress, mitochondrial dysfunction, defective axonal transport, neuroinflammation, altered energy metabolism, and recently RNA misprocessing [12, 103]. The fact that mitochondria are compromised in ALS is apparent from multiple studies performed using cellular or animal models of disease and in patients. Early studies on post-mortem tissues of ALS patients identified structural and morphological abnormalities in mitochondria of skeletal muscle, liver, spinal cord neurons and motor cortex at the electron microscopic level [104, 105]. Despite recent advances, the human mutant SOD1 remains the most studied ALS-associated gene and the SOD1G93A Tg mouse being the choice of disease model for pharmacological screening. Various mechanisms had been proposed by which mutant SOD1 exerts its toxicity on mitochondrial functions. Evidence indicates that mutant SOD1 directly interacts with Bcl-2, leading to exposure of the toxic BH3 domain, which in turn causes mitochondrial damage [106]. Protein misfolding and aggregation is common hallmark of numerous neurodegenerative diseases. Many FALS-link SOD1 mutants, including SOD1G93A, have an increased propensity to misfold due to specific alterations in their amino acid sequence, which in turn affects the dynamics and stability of the protein's tertiary structure [107]. Interestingly certain aberrant post-translational modifications can also cause wild type SOD1 to misfold as well. More recently, uptake of both misfolded mutant-SOD1 as well as aggregated mutant-SOD1 was shown to induce misfolding, and subsequently aggregation of the native wild type SOD1 protein [108]. Therefore, it has also been suggested that mutant SOD1 may alter wild type

SOD1's dismutase activity, presumably via this "prion-like" manner [108, 109], thus presenting a "gain in toxic function". This caused superoxide and ROS to build up in the respiring mitochondria of large alpha-motor neurons, which was mentioned earlier to be the more susceptible subtype. In synergy with the persistent activation of Nox2 and abnormally high levels of ROS from the alternation of the SOD1/Rac1 interaction [110], the fast motor neurons gradually die off due to accumulated oxidative stress. It has also been suggested that the defective axonal transport of mitochondria in SOD1G93A mouse is responsible for the "die-back" phenomena in which motor neurons retracts back from the neuromuscular junctions, breaking the communication with muscle fibers. As the glycolytic muscle fibers lose their connections with motor neuron, the slower small alpha-motor neurons may re-innervate these muscle fibers [68], resulting in the switching of ATP generation of the motor unit from glycolytic, to using oxidative phosphorylation. Since glycolysis has been shut down and the body goes into a state of hypermetabolism, alternative sources of acetyl-CoA (via β-oxidation of fatty acids, and ketone bodies) are needed to feed the TCA cycle, which in turns provides NADH and succinate to drive the electron transport chain to generate ATP via oxidative phosphorylation.

Our untargeted metabonomic approach confirmed that the downstream events of mitochondrial dysfunction associated with ALS can be profiled preclinically. These include changes in carbohydrate metabolism to signs of hypermetabolism. Such perturbation in energy metabolism may occur regardless of the initial cause of the disease, be it genetic via mutations, or sporadic. There is however a caveat in our study: the identities of the marker metabolites are at the moment putative. One of the important but challenging steps in metabonomics is the determination of the identities of marker metabolites [111]. Utmost effort has been put in to ensure that the identification of metabolites does not only rely on the level of electron impact (EI) spectral match, but also include RIs in order to optimize the quality and reliability of library hits [112]. RIs are the relative retention times (RRT)

normalized to adjacently eluting n-alkanes [113]. Although RT can vary with the individual chromatographic system, the RIs of metabolites are comparable between analytical laboratories under varying conditions [114]. It is however encouraging that in a recent publication, Lawton et al. employed a similar GC/MS human plasma profiling approach to profile ALS and detected a similar subset of marker metabolites [80]. Their findings therefore cross-validate. They identified a panel of 32 metabolites as biomarkers that differentiated ALS patients from disease mimics such as autoimmune motor neuropathy, spinal muscular atrophy, Kennedy's disease, cervical myelopathy, multiple sclerosis and hereditary spastic paraparesis [80]. Common pathways that were identified in the clinical study and our current preclinical study were energy, lipids, amino acids and nucleotides metabolisms. The specific metabolites that were identified in both studies were mainly the fatty acids (myristic acid, palmitic acid, cholesterol and DHA) and ketone bodies (3-hydroxybutyrate). However, the changes in the identified metabolites levels are not aligned: the fatty acids and ketone bodies in our study were found to be lower in the SOD1G93A Tg mice, however they were elevated in the plasma of ALS patients when compared against both patients of disease mimics and healthy subjects [80]. In the clinical study, the ALS patients were newly diagnosed; and furthermore, based on the reported ALS Functional Rating Scale (ALSFRS-R) scores [115], most of the patients were at an early stage in the disease progression when ALS is most difficult to diagnose; 75% of the patient ALSFRS-R scores were over 35 and only 4% of ALS patients enrolled in the study recorded scores of 24 or less. Usually, an ALSFRS-R score cut-off of 24 is used to distinguish high from low disease severity. In short, the plasma samples were derived from patients who are probably in the early stage of disease, or exhibited mild disease symptoms. In contrast, as this is a very first attempt to discern potential metabolic changes in a disease phenotype, we chose to use mice that were in the advanced stage of disease state for this current study (Table 1). This may explain the discrepancy in the relative expression of the respective metabolites. The

perturbation of energy metabolism however is in agreement in both studies; the decrease of inosine in our study (Table 3) and the decline in the levels of metabolites of xanthine metabolism in the clinical study [80] point to a reduction in ATP production and energy metabolism (Figure 4). The biomarker urate, an antioxidant, and the final product of xanthine metabolism, was lower in the plasma of ALS patients and was positively correlated with their ALSFRS-R scores, consistent with earlier reports [116, 117].

There has always been a concern about using the SOD1G93A Tg mouse model of ALS in the preclinical development of ALS intervention: whether results seen in the mouse model can be translated to human patients [20, 21]. Conventionally, pharmacodynamic assays have been performed with the disease models against healthy wild type controls. In our present study, we tried to eliminate any interference that can potentially come from the introduction of an exogenous gene into the mouse genome, by first excluding metabolite perturbation that is found between the 2 groups of healthy controls: the wild type strain-matched non-carrier and mouse carrying the normal human SOD1 gene. Given that there is a high degree of overlap in the pathways identified in both clinical and preclinical studies, and that in the clinical study, the patients showed different genetic backgrounds (i.e. patient population consists of both SALS, and FALS, of which, are not limited to the ones which were caused by mutations of the SOD1 gene), the common marker metabolites and perturbed pathways could be utilised preclinically to monitor disease progression and pharmacological effects with therapeutic interventions. With the findings by Lawton et al., this may also be an opportunity for a translatable pharmacodynamic model to be developed. The model may be utilized from the preclinical phase of drug discovery, to the clinical monitoring of effects of therapies on ALS patients. As such, future studies designed to represent the full range of ALS disease severity, preferably longitudinally, with proper validation of metabolites using analytical standards, could further explore the correlation of these biochemical pathways with disease progression. Additionally, an opportunity for subject stratification was

presented; of the 18 animals from the SOD1G93A Tg group, 6 showed impairments and/or paralysis of the lower limbs. It is possible for us to group these 6 mice as a separate class in attempt to further identify the metabolites that potentially differentiated these mice with apparent earlier onset of disease. Unfortunately, due to time factor, we did not manage to do it, but definitely something worth looking into even outside the content of this thesis. And if successful, it would no doubt be very exciting if this stratification of subjects by metabolite markers is translatable to the clinic as well. Lastly, our untargeted approach in metabolomics has rekindled the possibility of the central dopaminergic system being involved in this relentless disease and the search for new targets in this direction can be further explored.

6. References:

1. Rowland, L.P. and N.A. Shneider, *Amyotrophic lateral sclerosis.* N Engl J Med, 2001. **344**(22): p. 1688-700.

2. Andersen, P.M., *Amyotrophic lateral sclerosis associated with mutations in the CuZn superoxide dismutase gene.* Curr Neurol Neurosci Rep, 2006. **6**(1): p. 37-46.

3. Logroscino, G., et al., *Incidence of amyotrophic lateral sclerosis in Europe.* J Neurol Neurosurg Psychiatry, 2010. **81**(4): p. 385-90.

4. Marin, B., et al., *Incidence of amyotrophic lateral sclerosis in the Limousin region of France, 1997-2007.* Amyotroph Lateral Scler, 2009. **10**(4): p. 216-20.

5. Ragonese, P., et al., *Accuracy of death certificates for amyotrophic lateral sclerosis varies significantly from north to south of Italy: implications for mortality studies.* Neuroepidemiology, 2004. **23**(1-2): p. 73-7.

6. Sorenson, E.J., et al., *Amyotrophic lateral sclerosis in Olmsted County, Minnesota, 1925 to 1998.* Neurology, 2002. **59**(2): p. 280-2.

7. Logroscino, G., et al., *Descriptive epidemiology of amyotrophic lateral sclerosis: new evidence and unsolved issues.* J Neurol Neurosurg Psychiatry, 2008. **79**(1): p. 6-11.

8. Rowland, L.P., *How amyotrophic lateral sclerosis got its name: the clinical-pathologic genius of Jean-Martin Charcot.* Arch Neurol, 2001. **58**(3): p. 512-5.

9. Bosco, D.A. and J.E. Landers, *Genetic determinants of amyotrophic lateral sclerosis as therapeutic targets.* CNS Neurol Disord Drug Targets, 2010. **9**(6): p. 779-90.

10. Bento-Abreu, A., et al., *The neurobiology of amyotrophic lateral sclerosis.* Eur J Neurosci, 2010. **31**(12): p. 2247-65.

11. Rosen, D.R., et al., *Mutations in Cu/Zn superoxide dismutase gene are associated with familial amyotrophic lateral sclerosis.* Nature, 1993. **362**(6415): p. 59-62.

12. Vatovec, S., A. Kovanda, and B. Rogelj, *Unconventional features of C9ORF72 expanded repeat in amyotrophic lateral sclerosis and frontotemporal lobar degeneration.* Neurobiol Aging, 2014. **35**(10): p. 2421 e1-2421 e12.

13. Miller, R.G., J.D. Mitchell, and D.H. Moore, *Riluzole for amyotrophic lateral sclerosis (ALS)/motor neuron disease (MND).* Cochrane Database Syst Rev, 2012. **3**: p. CD001447.

14. Aggarwal, S. and M. Cudkowicz, *ALS drug development: reflections from the past and a way forward.* Neurotherapeutics, 2008. **5**(4): p. 516-27.

15. Gordon, P.H., *Amyotrophic Lateral Sclerosis: An update for 2013 Clinical Features, Pathophysiology, Management and Therapeutic Trials.* Aging Dis, 2013. **4**(5): p. 295-310.

16. Gurney, M.E., et al., *Motor neuron degeneration in mice that express a human Cu,Zn superoxide dismutase mutation.* Science, 1994. **264**(5166): p. 1772-5.

17. Bruijn, L.I., et al., *ALS-linked SOD1 mutant G85R mediates damage to astrocytes and promotes rapidly progressive disease with SOD1-containing inclusions.* Neuron, 1997. **18**(2): p. 327-38.

18. Synofzik, M., et al., *The human G93A SOD1 phenotype closely resembles sporadic amyotrophic lateral sclerosis.* J Neurol Neurosurg Psychiatry, 2010. **81**(7): p. 764-7.

19. Turner, B.J. and K. Talbot, *Transgenics, toxicity and therapeutics in rodent models of mutant SOD1-mediated familial ALS.* Prog Neurobiol, 2008. **85**(1): p. 94-134.

20. Nirmalananthan, N. and L. Greensmith, *Amyotrophic lateral sclerosis: recent advances and future therapies.* Curr Opin Neurol, 2005. **18**(6): p. 712-9.

21. Scott, S., et al., *Design, power, and interpretation of studies in the standard murine model of ALS.* Amyotroph Lateral Scler, 2008. **9**(1): p. 4-15.

22. Rothstein, J.D., *Of mice and men: reconciling preclinical ALS mouse studies and human clinical trials.* Ann Neurol, 2003. **53**(4): p. 423-6.

23. Lilo, E., et al., *Characterization of human sporadic ALS biomarkers in the familial ALS transgenic mSOD1G93A mouse model.* Hum Mol Genet, 2013.

24. Gurney, M.E., et al., *Benefit of vitamin E, riluzole, and gabapentin in a transgenic model of familial amyotrophic lateral sclerosis.* Ann Neurol, 1996. **39**(2): p. 147-57.

25. McGoldrick, P., et al., *Rodent models of amyotrophic lateral sclerosis.* Biochim Biophys Acta, 2013. **1832**(9): p. 1421-36.

26. Ganesalingam, J. and R. Bowser, *The application of biomarkers in clinical trials for motor neuron disease.* Biomark Med, 2010. **4**(2): p. 281-97.

27. Kaddurah-Daouk, R., B.S. Kristal, and R.M. Weinshilboum, *Metabolomics: a global biochemical approach to drug response and disease.* Annual review of pharmacology and toxicology, 2008. **48**: p. 653-83.

28. Nicholson, J.K., J.C. Lindon, and E. Holmes, *'Metabonomics': understanding the metabolic responses of living systems to pathophysiological stimuli via multivariate statistical analysis of biological NMR spectroscopic data.* Xenobiotica; the fate of foreign compounds in biological systems, 1999. **29**(11): p. 1181-9.

29. Fiehn, O., *Metabolomics--the link between genotypes and phenotypes.* Plant molecular biology, 2002. **48**(1-2): p. 155-71.

30. Martin, F.P., et al., *A top-down systems biology view of microbiome-mammalian metabolic interactions in a mouse model.* Mol Syst Biol, 2007. **3**: p. 112.

31. Hood, L., et al., *Systems biology and new technologies enable predictive and preventative medicine.* Science (New York, N.Y.), 2004. **306**(5696): p. 640-3.

32. Kaddurah-Daouk, R. and K.R. Krishnan, *Metabolomics: a global biochemical approach to the study of central nervous system diseases.* Neuropsychopharmacology, 2009. **34**(1): p. 173-86.

33. Quinones, M.P. and R. Kaddurah-Daouk, *Metabolomics tools for identifying biomarkers for neuropsychiatric diseases.* Neurobiol Dis, 2009. **35**(2): p. 165-76.

34. Niessen, H.G., et al., *Metabolic progression markers of neurodegeneration in the transgenic G93A-SOD1 mouse model of amyotrophic lateral sclerosis.* Eur J Neurosci, 2007. **25**(6): p. 1669-77.

35. Suhy, J., et al., *Early detection and longitudinal changes in amyotrophic lateral sclerosis by (1)H MRSI.* Neurology, 2002. **58**(5): p. 773-9.

36. Abe, K., et al., *Decrease in N-acetylaspartate/creatine ratio in the motor area and the frontal lobe in amyotrophic lateral sclerosis.* Neuroradiology, 2001. **43**(7): p. 537-41.

37. Block, W., et al., *Proton magnetic resonance spectroscopy of the primary motor cortex in patients with motor neuron disease: subgroup analysis and follow-up measurements.* Arch Neurol, 1998. **55**(7): p. 931-6.

38. Tsai, C.F., et al., *Differences in Brain Metabolism Associated with Agitation and Depression in Alzheimer's disease.* East Asian Arch Psychiatry, 2013. **23**(3): p. 86-90.

39. Tae, W.S., et al., *Progressive decrease of N-acetylaspartate to total creatine ratio in the pregenual anterior cingulate cortex in patients with major depressive disorder: longitudinal 1H-MR spectroscopy study.* Acta Radiol, 2013.

40. Cagnoli, P., et al., *Reduced Insular Glutamine and N-acetylaspartate in systemic lupus erythematosus: a single-voxel (1)H-MR spectroscopy study.* Acad Radiol, 2013. **20**(10): p. 1286-96.

41. Achtnichts, L., et al., *Global N-acetylaspartate concentration in benign and non-benign multiple sclerosis patients of long disease duration.* Eur J Radiol, 2013.

42. Ramos-Zuniga, R., et al., *Post concussion syndrome and mild head injury. The role of early diagnosis using Neuropsychological test and fMR/spectroscopy.* World Neurosurg, 2013.

43. Blasco, H., et al., *1H-NMR-based metabolomic profiling of CSF in early amyotrophic lateral sclerosis.* PLoS One, 2010. **5**(10): p. e13223.

44. Kumar, A., et al., *Metabolomic analysis of serum by (1) H NMR spectroscopy in amyotrophic lateral sclerosis.* Clin Chim Acta, 2010. **411**(7-8): p. 563-7.

45. Atherton, H.J., et al., *A combined 1H-NMR spectroscopy- and mass spectrometry-based metabolomic study of the PPAR-alpha null mutant mouse defines profound systemic changes in metabolism linked to the metabolic syndrome.* Physiol Genomics, 2006. **27**(2): p. 178-86.

46. Pasikanti, K.K., P.C. Ho, and E.C. Chan, *Gas chromatography/mass spectrometry in metabolic profiling of biological fluids.* J Chromatogr B Analyt Technol Biomed Life Sci, 2008. **871**(2): p. 202-11.

47. Want, E.J., et al., *From exogenous to endogenous: the inevitable imprint of mass spectrometry in metabolomics.* J Proteome Res, 2007. **6**(2): p. 459-68.

48. Wuolikainen, A., et al., *Disease-related changes in the cerebrospinal fluid metabolome in amyotrophic lateral sclerosis detected by GC/TOFMS.* PLoS One, 2011. **6**(4): p. e17947.

49. Wuolikainen, A., et al., *ALS patients with mutations in the SOD1 gene have an unique metabolomic profile in the cerebrospinal fluid compared with ALS patients without mutations.* Mol Genet Metab, 2012. **105**(3): p. 472-8.

50. Ludolph, A.C., et al., *Guidelines for the preclinical in vivo evaluation of pharmacological active drugs for ALS/MND: report on the 142nd ENMC international workshop.* Amyotroph Lateral Scler, 2007. **8**(4): p. 217-23.

51. Ludolph, A.C., et al., *Guidelines for preclinical animal research in ALS/MND: A consensus meeting.* Amyotroph Lateral Scler, 2010. **11**(1-2): p. 38-45.

52. Chan, E.C., K.K. Pasikanti, and J.K. Nicholson, *Global urinary metabolic profiling procedures using gas chromatography-mass spectrometry.* Nat Protoc, 2011. **6**(10): p. 1483-99.

53. Koh, Y., et al., *Comparative evaluation of software for retention time alignment of gas chromatography/time-of-flight mass spectrometry-based metabonomic data.* J Chromatogr A, 2010. **1217**(52): p. 8308-16.

54. Kopka, J., et al., *GMD@CSB.DB: the Golm Metabolome Database.* Bioinformatics, 2005. **21**(8): p. 1635-8.

55. Wishart, D.S., et al., *HMDB 3.0--The Human Metabolome Database in 2013.* Nucleic Acids Res, 2013. **41**(Database issue): p. D801-7.

56. Xia, J., et al., *MetaboAnalyst 2.0--a comprehensive server for metabolomic data analysis.* Nucleic Acids Res, 2012. **40**(Web Server issue): p. W127-33.

57. Kanehisa, M. and S. Goto, *KEGG: kyoto encyclopedia of genes and genomes.* Nucleic Acids Res, 2000. **28**(1): p. 27-30.

58. Want, E.J., et al., *Global metabolic profiling procedures for urine using UPLC-MS.* Nat Protoc, 2010. **5**(6): p. 1005-18.

59. Koerner, D.R., *Abnormal carbohydrate metabolism in amyotrophic lateral sclerosis and Parkinsonism-dementia on Guam.* Diabetes, 1976. **25**(11): p. 1055-65.

60. Pradat, P.F., et al., *Impaired glucose tolerance in patients with amyotrophic lateral sclerosis.* Amyotroph Lateral Scler, 2010. **11**(1-2): p. 166-71.

61. Poulton, K.R. and M.L. Rossi, *Peripheral nerve protein glycation and muscle fructolysis: evidence of abnormal carbohydrate metabolism in ALS.* Funct Neurol, 1993. **8**(1): p. 33-42.

62. Dupuis, L. and J.P. Loeffler, *Neuromuscular junction destruction during amyotrophic lateral sclerosis: insights from transgenic models.* Curr Opin Pharmacol, 2009. **9**(3): p. 341-6.

63. Pun, S., et al., *Selective vulnerability and pruning of phasic motoneuron axons in motoneuron disease alleviated by CNTF.* Nat Neurosci, 2006. **9**(3): p. 408-19.

64. Hegedus, J., C.T. Putman, and T. Gordon, *Time course of preferential motor unit loss in the SOD1 G93A mouse model of amyotrophic lateral sclerosis.* Neurobiol Dis, 2007. **28**(2): p. 154-64.

65. Schmied, A., J. Pouget, and J.P. Vedel, *Electromechanical coupling and synchronous firing of single wrist extensor motor units in sporadic amyotrophic lateral sclerosis.* Clin Neurophysiol, 1999. **110**(5): p. 960-74.

66. Atkin, J.D., et al., *Properties of slow- and fast-twitch muscle fibres in a mouse model of amyotrophic lateral sclerosis.* Neuromuscul Disord, 2005. **15**(5): p. 377-88.

67. Gordon, T., et al., *Functional over-load saves motor units in the SOD1-G93A transgenic mouse model of amyotrophic lateral sclerosis.* Neurobiol Dis, 2010. **37**(2): p. 412-22.

68. Sharp, P.S., J.R. Dick, and L. Greensmith, *The effect of peripheral nerve injury on disease progression in the SOD1(G93A) mouse model of amyotrophic lateral sclerosis.* Neuroscience, 2005. **130**(4): p. 897-910.

69. Desport, J.C., et al., *Hypermetabolism in ALS: correlations with clinical and paraclinical parameters.* Neurodegener Dis, 2005. **2**(3-4): p. 202-7.

70. Bouteloup, C., et al., *Hypermetabolism in ALS patients: an early and persistent phenomenon.* J Neurol, 2009. **256**(8): p. 1236-42.

71. Desport, J.C., et al., *Factors correlated with hypermetabolism in patients with amyotrophic lateral sclerosis.* Am J Clin Nutr, 2001. **74**(3): p. 328-34.

72. Ahmed, R.M., et al., *Body mass index delineates ALS from FTD: implications for metabolic health.* J Neurol, 2014.

73. Desport, J.C., et al., *Nutritional assessment and survival in ALS patients.* Amyotroph Lateral Scler Other Motor Neuron Disord, 2000. **1**(2): p. 91-6.

74. Kasarskis, E.J., et al., *Nutritional status of patients with amyotrophic lateral sclerosis: relation to the proximity of death.* Am J Clin Nutr, 1996. **63**(1): p. 130-7.

75. Jung, C., C.M. Higgins, and Z. Xu, *Mitochondrial electron transport chain complex dysfunction in a transgenic mouse model for amyotrophic lateral sclerosis.* J Neurochem, 2002. **83**(3): p. 535-45.

76. Dupuis, L., et al., *Evidence for defective energy homeostasis in amyotrophic lateral sclerosis: benefit of a high-energy diet in a transgenic mouse model.* Proc Natl Acad Sci U S A, 2004. **101**(30): p. 11159-64.

77. Fergani, A., et al., *Increased peripheral lipid clearance in an animal model of amyotrophic lateral sclerosis.* J Lipid Res, 2007. **48**(7): p. 1571-80.

78. Guzman, M. and C. Blazquez, *Ketone body synthesis in the brain: possible neuroprotective effects.* Prostaglandins Leukot Essent Fatty Acids, 2004. **70**(3): p. 287-92.

79. Yi, C.X., et al., *A role for astrocytes in the central control of metabolism.* Neuroendocrinology, 2011. **93**(3): p. 143-9.

80. Lawton, K.A., et al., *Plasma metabolomic biomarker panel to distinguish patients with amyotrophic lateral sclerosis from disease mimics.* Amyotroph Lateral Scler Frontotemporal Degener, 2014: p. 1-9.

81. Connolly, G.P. and J.A. Duley, *Uridine and its nucleotides: biological actions, therapeutic potentials.* Trends Pharmacol Sci, 1999. **20**(5): p. 218-25.

82. Wurtman, R.J., et al., *Effect of oral CDP-choline on plasma choline and uridine levels in humans.* Biochem Pharmacol, 2000. **60**(7): p. 989-92.

83. Wurtman, R.J., et al., *Use of phosphatide precursors to promote synaptogenesis.* Annu Rev Nutr, 2009. **29**: p. 59-87.

84. Cansev, M., *Uridine and cytidine in the brain: their transport and utilization.* Brain Res Rev, 2006. **52**(2): p. 389-97.

85. Ipata, P.L., et al., *Metabolic interplay between intra- and extra-cellular uridine metabolism via an ATP driven uridine-UTP cycle in brain.* Int J Biochem Cell Biol, 2010. **42**(6): p. 932-7.

86. Amante, D.J., et al., *Uridine ameliorates the pathological phenotype in transgenic G93A-ALS mice.* Amyotroph Lateral Scler, 2010. **11**(6): p. 520-30.

87. Olgun, A. and S. Akman, *Mitochondrial DNA-deficient models and aging.* Ann N Y Acad Sci, 2007. **1100**: p. 241-5.

88. Khakh, B.S. and G. Burnstock, *The double life of ATP.* Sci Am, 2009. **301**(6): p. 84-90, 92.

89. Fitz, J.G., *Regulation of cellular ATP release.* Trans Am Clin Climatol Assoc, 2007. **118**: p. 199-208.

90. Surprenant, A. and R.A. North, *Signaling at purinergic P2X receptors.* Annu Rev Physiol, 2009. **71**: p. 333-59.

91. Fischer, W. and U. Krugel, *P2Y receptors: focus on structural, pharmacological and functional aspects in the brain.* Curr Med Chem, 2007. **14**(23): p. 2429-55.

92. Fredholm, B.B., *Adenosine, an endogenous distress signal, modulates tissue damage and repair.* Cell Death Differ, 2007. **14**(7): p. 1315-23.

93. Mizuno, Y., et al., *Clinical efficacy of istradefylline (KW-6002) in Parkinson's disease: a randomized, controlled study.* Mov Disord, 2010. **25**(10): p. 1437-43.

94. Friedle, S.A., M.A. Curet, and J.J. Watters, *Recent patents on novel P2X(7) receptor antagonists and their potential for reducing central nervous system inflammation.* Recent Pat CNS Drug Discov, 2010. **5**(1): p. 35-45.

95. van Kuilenburg, A.B., et al., *Analysis of pyrimidine synthesis "de novo" intermediates in urine and dried urine filter- paper strips with HPLC-electrospray tandem mass spectrometry.* Clin Chem, 2004. **50**(11): p. 2117-24.

96. Zhao, S., et al., *Muscle adenine nucleotide metabolism during and in recovery from maximal exercise in humans.* J Appl Physiol (1985), 2000. **88**(5): p. 1513-9.

97. Testa, D., et al., *Decreased CSF levels of homovanillic acid in ALS patients.* Eur J Neurol, 1995. **2**(1): p. 27-9.

98. Andreassen, O.A., et al., *Transgenic ALS mice show increased vulnerability to the mitochondrial toxins MPTP and 3-nitropropionic acid.* Exp Neurol, 2001. **168**(2): p. 356-63.

99. Machteld Marcelisa, J.S., Paul Hofman, Peter Woodruff, Ed Bullmore, Jim van Os, *Evidence that brain tissue volumes are associated with HVA reactivity to metabolic stress in schizophrenia.* Schizophrenia Research, 2006. **86**(1-3): p. 9.

100. Breier, A., et al., *Effects of metabolic perturbation on plasma homovanillic acid in schizophrenia. Relationship to prefrontal cortex volume.* Arch Gen Psychiatry, 1993. **50**(7): p. 541-50.

101. Breier, A., *A.E. Bennett award paper. Experimental approaches to human stress research: assessment of neurobiological mechanisms of stress in volunteers and psychiatric patients.* Biol Psychiatry, 1989. **26**(5): p. 438-62.

102. Hartikainen, P., et al., *Neurochemical markers in the cerebrospinal fluid of patients with Alzheimer's disease, Parkinson's disease and amyotrophic lateral sclerosis and normal controls.* J Neural Transm Park Dis Dement Sect, 1992. **4**(1): p. 53-68.

103. Ling, S.C., M. Polymenidou, and D.W. Cleveland, *Converging mechanisms in ALS and FTD: disrupted RNA and protein homeostasis.* Neuron, 2013. **79**(3): p. 416-38.

104. Sasaki, S. and M. Iwata, *Ultrastructural change of synapses of Betz cells in patients with amyotrophic lateral sclerosis.* Neurosci Lett, 1999. **268**(1): p. 29-32.

105. Menzies, F.M., et al., *Mitochondrial dysfunction in a cell culture model of familial amyotrophic lateral sclerosis.* Brain, 2002. **125**(Pt 7): p. 1522-33.

106. Pasinelli, P., et al., *Amyotrophic lateral sclerosis-associated SOD1 mutant proteins bind and aggregate with Bcl-2 in spinal cord mitochondria.* Neuron, 2004. **43**(1): p. 19-30.

107. Rotunno, M.S. and D.A. Bosco, *An emerging role for misfolded wild-type SOD1 in sporadic ALS pathogenesis.* Front Cell Neurosci, 2013. **7**: p. 253.

108. Sundaramoorthy, V., et al., *Extracellular wildtype and mutant SOD1 induces ER-Golgi pathology characteristic of amyotrophic lateral sclerosis in neuronal cells.* Cell Mol Life Sci, 2013. **70**(21): p. 4181-95.

109. Vehvilainen, P., J. Koistinaho, and G. Gundars, *Mechanisms of mutant SOD1 induced mitochondrial toxicity in amyotrophic lateral sclerosis.* Front Cell Neurosci, 2014. **8**: p. 126.

110. Harraz, M.M., et al., *SOD1 mutations disrupt redox-sensitive Rac regulation of NADPH oxidase in a familial ALS model.* J Clin Invest, 2008. **118**(2): p. 659-70.

111. Wishart, D.S., et al., *HMDB: the Human Metabolome Database.* Nucleic Acids Res, 2007. **35**(Database issue): p. D521-6.

112. Halket, J.M., et al., *Chemical derivatization and mass spectral libraries in metabolic profiling by GC/MS and LC/MS/MS.* J Exp Bot, 2005. **56**(410): p. 219-43.

113. Vandendool, H. and P.D. Kratz, *A Generalization of the Retention Index System Including Linear Temperature Programmed Gas-Liquid Partition Chromatography.* J Chromatogr, 1963. **11**: p. 463-71.

114. Kind, T., et al., *FiehnLib: mass spectral and retention index libraries for metabolomics based on quadrupole and time-of-flight gas chromatography/mass spectrometry.* Anal Chem, 2009. **81**(24): p. 10038-48.

115. Cedarbaum, J.M., et al., *The ALSFRS-R: a revised ALS functional rating scale that incorporates assessments of respiratory function. BDNF ALS Study Group (Phase III).* J Neurol Sci, 1999. **169**(1-2): p. 13-21.

116. Ikeda, K., et al., *Relationships between disease progression and serum levels of lipid, urate, creatinine and ferritin in Japanese patients with amyotrophic lateral sclerosis: a cross-sectional study.* Intern Med, 2012. **51**(12): p. 1501-8.

117. Keizman, D., et al., *Low uric acid levels in serum of patients with ALS: further evidence for oxidative stress?* J Neurol Sci, 2009. **285**(1-2): p. 95-9.